Hierarchically Bimodal Porous Metallosilicate Catalysts for Acetolysis of Epichlorohydrin

EMIL IOAN MURESAN[1]*, ADRIAN PUITEL[1], AUREL PUI[2], CEZAR DORU RADU[3]*, DANIEL TAMPU[4], NICANOR CIMPOIESU[5], ION SANDU[6,7]

[1]Gheorghe Asachi Technical University, Faculty of Chemical Engineering and Environmental Protection, 73 Mangeron Blvd., 700050, Iasi, Romania

[2]Alexandru Ioan Cuza University, Faculty of Chemistry, 11 Carol I Blvd., 700050, Iasi, Romania

[3] Gheorghe Asachi Technical University, Faculty of Textiles, Leather Engineering and Industrial Management, 29 Mangeron Blvd., 700050, Iasi, Romania

[4]Institute of Macromolecular Chemistry Petru Poni,41A Grigore Ghica Voda Alley, 700487, Iasi, Romania

[5]Gheorghe Asachi Technical University, Faculty of Materials Science and Engineering, 41 Mangeron Blvd., 700050, Iasi, Romania

[6] Alexandru Ioan Cuza University, ARHEOINVEST Interdisciplinary Platform, 11 Carol I Bvd., Corp G demisol, 700506, Iasi,Romania

[7] Alexandru Ioan Cuza University, Faculty of Biology, 11 Carol I Blvd., 700506, Ia^{o}i, Romania

The aim of this work was to prepare macrospherical catalysts which are easy to handle, recover and reuse. The metallosilicate macrospheres were obtained by incorporation of Ce(IV), Cr(III) and Zr within the silica framework using tetraethyl orthosilicate as silicon source. The yeast cells and chitosan were used as templates to generate the hierarchical multimodal porosity of the inorganic materials. The synthesized materials were characterized by water sorption technique, FTIR spectroscopy, DRX and SEM/EDAX analyses. Catalytic activity of the obtained metallosilicate macrospheres was analyzed in the acetolysis reaction of epichlorohydrin.

Keywords: metallosilicate macrospheres, yeast cells, chitosan, heterogeneous catalysis,bimodal porous materials

The esterification reaction of carboxylic acids with epichlorohydrin has been extensively studied due to the simplicity of technology, accessibility of the reactants and practical significance of the products obtained. Thus, the hydroxyalkyl esters of acetic acid are used as coating agents for low temperature processes, solvents for dyeing compositions, cement modifiers and components of anticorrosive coatings.

In the addition reaction of acetic acid to epichlorohydrin two isomeric esters are formed (scheme 1): 3-chloro-2-hydroxypropyl acetate (also known as the normal ester) and 3-chloro-1-hydroxypropyl acetate (the abnormal ester).

The regioselectivity of ring opening mainly depends on the kind of catalyst and temperature of reaction. A variety of homogeneous catalysts such as alkaline hydroxides, alkaline salts of organic acids, quaternary ammonium salts, complexes of transition metals were tested in the esterification reaction of carboxylic acids to epichlorohydrin [1-13]. The use of heterogeneous catalysts (ion exchange resins, zeolites, mesoporous materials) confer numerous advantages such as: easy separation from the reaction mixture through filtration or decantation, possibility of reusing the catalyst, avoiding the use of corrosive materials (acids, bases) as catalysts [14-16].

In the last decades the incorporation of metallic ions within the silica framework became an efficient method for the manufacturing of heterogeneous catalysts. The valence, electronegativity, size, nature of the introduced metal atom significantly affects the properties and stability of the resulting materials [17-34]. However, the most of these materials are synthesized in powder form which makes difficult their separation from the reaction mixture.

The aim of this work was to test the effectiveness of macrospherical metallosilicate catalysts obtained by incorporation of Ce(IV), Cr(III) and Zr(IV) within the silica framework using tetraethyl orthosilicate as silicon source. The yeast cells and chitosan were used as templates to generate the hierarchical multimodal porosity of the inorganic materials.

Experimental part

Materials and Methods

Chemicals

Epichlorohydrin (ECH) and acetic acid were commercial samples from Merck and were used without further purification. Chromium (III) nitrate, cerium (IV) sulphate and zirconium oxychloride, sodium hydroxide, bromothymol blue ($C_{27}H_{28}Br_2O_5S$), tetraethylorthosilicate (TEOS) were purchased from Aldrich.

Catalyst preparation

The porous metallosilicate macrospheres were prepared as follows: x g $Cr(NO_3)_3 \cdot 9H_2O$, y g $Ce(SO_4)_2$, 0.237 g $ZrOCl_2$

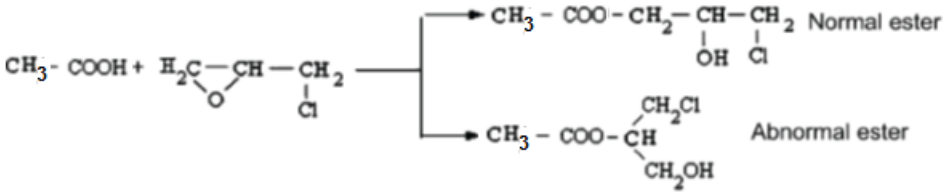

Scheme 1. Esterification reaction between acetic acid and epichlorohydrin

* email: eimuresan@yahoo.co.uk; dcradu@tex.tuiasi.ro

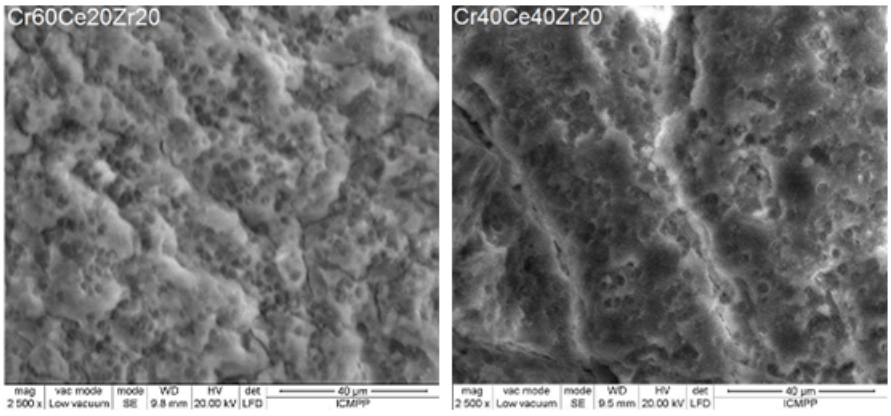

Fig.1. Scanning electron micrograph images of the catalysts

. $8H_2O$ and 0.6 mL HNO_3 98%, were introduced in 11 mL deionised water (where x = 0.8832 g and y = 0.24435 g for Cr60Ce20Zr20 catalyst type, x = 0.5888 g and y = 0.4887 g for Cr40Ce40Zr20 catalyst type). The mixture was vigorously stirred until complete homogenization. Then 3.75 mL tetraethyl orthosilicate were added and the stirring continued for 8 h at room temperature. Afterwards 7.3 g yeast cells suspension (3.8 g yeast cells and 3.5 mL of water were heated at 85°C for 2 h in order to inactivate the yeast cells and spores) and 6.25 g chitosan solution (0.25 g chitosan dissolved in 6 g acetic acid solution 4%) were added and the stirring was continued for another 2,5 h. The gel obtained was dropped with a syringe pump into a precipitation bath containing an ammonia solution (25%). The hybrid macrospheres were formed immediately when drops of gel fell down in the ammonia solution. The macrospheres were kept into ammonia solution for 40 min in order to harden. The obtained macrospheres were separated by filtration in a Buchner funnel and then were dried at 40°C for 24 h. The dried samples were calcined in air at 625°C for 24 h (increasing the temperature with a heating rate of 1°C/min) for the removal of the template. In order to remove the non-framework metallic ions the calcined samples were washed with distilled water (90°C), then with 20% acetic acid solution (90°C).

Characterization of the synthesized materials

Adsorption/desorption isotherms were recorded using an automated gravimetric analyzer IGAsorp supplied by Hiden Analytical, Warrington (UK). Scanning electron microscopy (SEM) and energy-dispersive X-ray (EDX) analyses were carried out using a VegaTescan LMHII (VegaTescan) scanning electron microscope coupled with an energy dispersive X-ray analyzer (Bruker XFlash 6/10 SDD with Esprit Software). The FTIR spectra were performed with aVertex 70 (Bruker) FTIR spectrometer using the conventional KBr-disk technique.

X-ray diffraction patterns were obtained with a Philips X PERT MPD (40 KV, 100 mA) diffractometer using a nickel-filtered Cu K± radiation (λ = 0.15418 nm). The instrument was operated in continuous mode at a generator tension of 40 kV and a generator current of 100 mA. The small angle X-ray diffraction measurements were recorded for a 2θ angle from 0.7 to 10° with a step size of 0.02 and a step time of 2 s.The wide angle X-ray diffraction measurements were performed in the 2θ range of 10-80° at a scanning speed of 1°/min. To allow the low angle measurements the 0.1° receiving slit in the diffractometer was replaced by a 0.25° one. The evaluation of the diffractograms was made with the DIFFRAC/AT software.

Procedure

Acetic acid and epichlorohydrin were placed in a round-bottom flask and heated to the desired temperature. Finally a given amount of catalyst was added. This was taken as zero time of the reaction. The reaction temperature was controlled using a thermocouple with digital temperature controller.The analysis of reaction mixture was carried out by gas chromatography using a Hewlet Packard 6890 chromatograph. A HP-1 column (30m length, 0.32 mm diameter, 0.17 μm film thickness) was used for separating the reactants and products. The conditions of GC analysis were: oven temperature program 50(3)-10-250, amount of sample injected 0.5 μL, carrier gas Helium, detector temperature 250°C. The identification of reaction products was carried out on a GS-MS QMD coupling. The external standard method was used to calculate the concentrations of components. 0.015 g sample of reaction mixture was dissolved in 5 mL of acetone and 0.1 μL of solution was injected into the gas chromatograph for analysis.

Characterization techniques

Scanning electron microscopy (SEM) and energy-dispersive X-ray (EDX) analyses

SEM images in high magnification of the two catalysts (fig.1) prove the presence of macropores that are benefic for the mass transport of reactants towards the catalytic centers.

The chemical composition of each sample was established using an energy-dispersive X-ray spectrometer attached to the SEM. The calculated metal/silicon ratios are listed in table 1.

A high amount of metals was incorporated within the silica framework (the percentage of incorporation was 86% for Cr60Ce20Zr20 catalyst and respectively 82% for Cr40Ce40Zr20 catalyst).

FTIR Analyses

Vibrations of the frameworks of zeolites give rise to typical bands in the mid and far infrared. A distinction occurs between external and internal vibrations of the elementary unit. The internal vibrations are stretches associated with movements within the elementary unit that comprise the zeolitic structure. These movements can be O–T–O bending modes or symmetric and asymmetric stretches of O–T–O bonds. The vibrations between adjacent

Catalyst	Metal : silicon ratios					
	Cr/Si		Ce/Si		Zr/Si	
	Input	Output	Input	Output	Input	Output
Cr60	0.1368	0.1256	0.0439	0.0354	0.0439	0.0328
Cr40	0.0878	0.0799	0.0878	0.0608	0.0439	0.0393

Table 1
METAL/ SILICON RATIOS FOR THE SYNTHESIZED SAMPLES

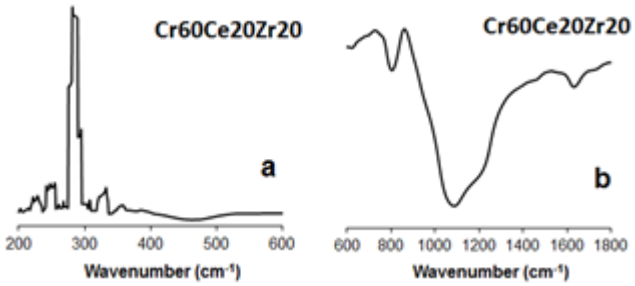

Fig. 2. FTIR spectra of Cr60Ce20Zr20 catalyst

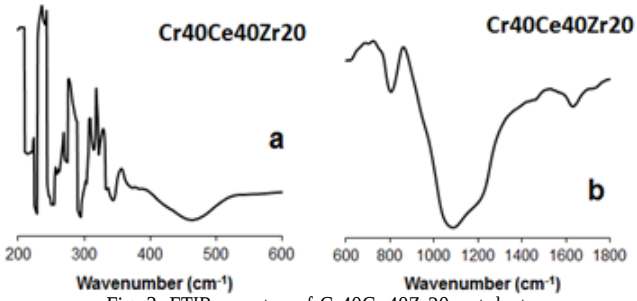

Fig. 3. FTIR spectra of Cr40Ce40Zr20 catalyst

elementary units include pore-opening vibrations of bonds between the oxygen atoms from the ring (also known as breathing mode) and ring opening mode.

The vibrational spectra in the far and mid infrared regions of the synthesized samples are shown in figure 2 and figure 3.

The peak at 462 cm^{-1} is assigned to the overlapping of bending mode vibrations of Si – O – Si and Si – O – M bonds. The symmetric stretching vibrations of Si – O – Si and Si – O – M bonds occur at 807 cm^{-1} (for Cr60Ce20Zr20 catalyst) and respectively at 806 cm^{-1} (for Cr40Ce40Zr20 catalyst). Peaks at 1086 cm^{-1} (Cr60Ce20Zr20 catalyst) and respectively 1082 cm^{-1} (Cr40Ce40Zr20 catalyst) are attributed to the overlapping of asymmetric stretching vibrations of Si – O – Si and Si – O – M bonds. The signals detected at 1633 cm^{-1}(Cr60Ce20Zr20 sample) and 1634 cm^{-1} (Cr40Ce40Zr20 sample) are related to the bending mode vibrations of the adsorbed water molecules. The broad bands around 3454 cm^{-1} and 3440 $cm^{-1}$for Cr60Ce20Zr20 catalyst and respectively Cr40Ce40Zr20 catalyst (not shown here) are assigned to the – OH stretching vibrations of bridging OH groups.

The peaks detected at 333 $cm^{-1}$for Cr60Ce20Zr20 catalyst and respectively at 317 $cm^{-1}$for Cr40Ce40Zr20 catalyst are attributed to the asymmetric stretching vibrations of bridging bonds Si-O-M between (SiO) tetrahedrons and (MO) primary units.The strong signals detected at 284 cm^{-1} (Cr60Ce20Zr20 sample) and 237 cm^{-1} (Cr40Ce40Zr20sample) represent the symmetric stretching vibrations of bridging bonds Si-O-M between (SiO) tetrahedrons and (MO) primary units. The peaks at 358 cm^{-1} (Cr60Ce20Zr20 sample) and respectively 357 cm^{-1}(Cr40Ce40Zr20 sample) are ascribed to the bending mode vibrations of O-M-O and O-Si-O external linkages.The translational mode of the water molecules corresponds to the bands at 208 cm^{-1} (Cr60Ce20Zr20 sample) and respectively 226 cm^{-1} (Cr40Ce40Zr20 sample). The characteristic band positions of the so-called pseudo-lattice vibrations (that occur in the range of 800–300 cm) shift toward lower wavenumbers in the IR spectra with the increase in number of ring members.

XRD analyses

The small-angle X-ray scattering (SAXS) spectra of the two catalysts are shown in figure 4.

In both XRD patterns one notices a single broad diffraction peak centered at the 2θ angle of 1.36° (for Cr60Ce20Zr20 catalyst) and respectively 1.291° (for Cr40Ce40Zr20 catalyst), which correspond to interplanar d-spacings of 64.91 Å (for Cr60Ce20Zr20 catalyst) and respectively 68.37Å (for Cr40Ce40Zr20 catalyst) as result from the Bragg equation ($2d \sin\theta = \lambda$, where λ = 1.5406Å for the Cu Kα line). The broadness of the single peak in the low angle range and the absence of additional higher degree peaks suggest that this sample lacks the long-range ordering in structure.

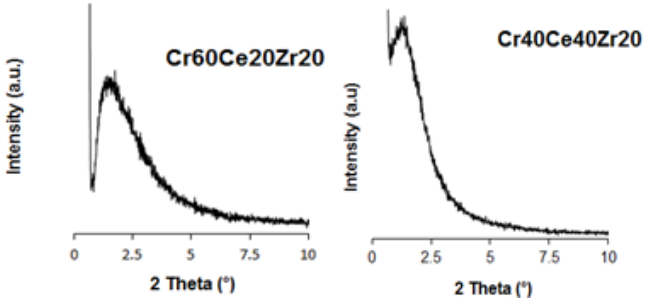

Fig.4. Small angle XRD patterns of the catalysts

Wide angle X-ray diffraction analysis is a frequently used technique to characterize the crystallinity and the phase purity of the materials. In figure 5 are shown the wide angle X-ray diffraction spectra of the two samples.

The wide angle XRD patterns of the metallosilicate catalysts present a broad and high peak centered at $2\theta \approx 22°$ characteristic to an amorphous material and many other peaks with low intensities (which correspond to crystalline phases). The broadness of these low peaks suggest that the crystallites have small dimensions.

Water isotherms

Water adsorption isotherms and pore size distributions are shown in figure 6.

The surface areas of the two catalysts were calculated using the Brunauer-Emmett-Teller (BET) method based on the adsoption data in the partial pressure (p/p_0) range 0.05 – 0.35. The pore size distribution was estimated using the Barrett-Joyner-Halenda (BJH) method.The application of the t plot method to the adsorption isotherms of both catalysts indicates that they do not present micropores. The total mesopore volume was obtained from the amount of water adsorbed at p/p_0 = 0.84. All the samples show broad hysteresis loops, indicating the presence of hierarchical mesopores/ macropores.

From figure 6 it is obvious, that the pore size distribution is quite broad beginning at 23 Å and ending at 120Å. The adsorption branch rise steeply with the increase of relative presure at relative humidities higher than 75%. According to the IUPAC classification of physisorption isotherms, the samples exhibit type IV isotherms with H_2 type hysteresis loops.

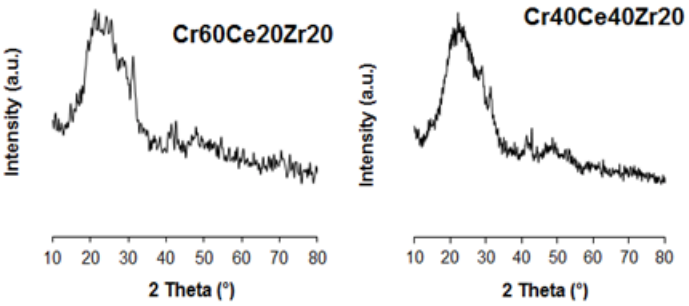

Fig. 5.Wide angle XRD patterns of the catalysts

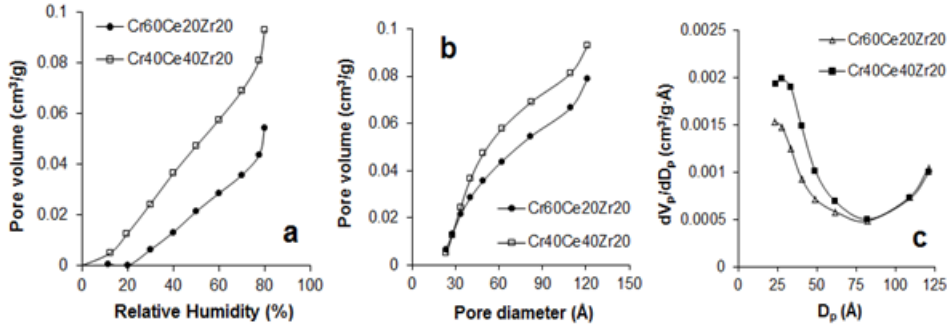

Fig.6. Adsorption branches of water isotherms and mesopore size distributions

The SEM images and adsorption isotherms indicate that the samples contain some larger mesopores and macropores which cannot be determined by water physisorption. The mesopore and macropore volumes, which could not be measured by water adsorption, were characterized using pycnometric methods. Skeletal densities were measured using a Micromimetics Helium AccuPyc 1330 pycnometer. The apparent densities were determined by mercury pynometry [34-40]. The textural properties of the two catalysts are listed in table 2.

Catalytic activity of metallosilicate beads in the reaction of acetic acid with epichlorohydrin

Preliminary experiments were conducted to select the optimal reaction parameters such as catalyst weight, mole ratio between reactants and reaction temperature. After each experiment, the composition of the final reaction mixture was analysed by gas chromatography. Besides the two isomeric esters (3-chloro-2-hydroxypropyl acetate and 1-chloromethyl-2-hydroxyethyl acetate) which are the main reaction products, the presence of the following byproducts was detected: dichlorohydroxypropane and glycidyl acetate (formed by dehydrochlorination of 3-chloro-2-hydroxyethyl acetate with epichlorohydrin), the products of addition of chlorohydroxyalkyl acetates to epichlorohydrin and glycerol diacetate (resulted from the reaction of glycidyl acetate with acetic acid).

The increase of catalyst content to more than 20% (w/w) does not markedily improve the conversion or reduce the reaction time. The dose of 15% (w/w) catalyst reported to the weight of the reaction mixture seems to be resonable and therefore this was the catalyst loading used in all experiments.The effect of mole ratio between reactants, reaction temperature and catalyst on the yields of the two isomeric hydroxypropyl esters is summarized in table 3.

The catalytic activity and regioselectivity are strongly affected by temperature and mole ratio between acetic acid and epichlorohydrin, while the catalyst exerts a slight influence.

At lower temperatures the reaction times were larger, but the yields in chlorohydroxypropyl esters were higher. A high selectivity was obtained for the experiments carried out at 75°C because the main esterification reaction performs very fast, while the side etherification reaction (addition of chlorohydroxyalkyl esters to epichlorohydrin) is slow.Except for a small quantity of glycidyl acetate and dichlorohydrin, only the main reaction products (3-chloro-2-hydroxypropyl acetate and 1-chloromethyl-2-hydroxyethyl acetate) were identified in the final reaction mixture.

In the experiments carried out at higher temperatures (85 and 95°C) the yields of normal and abnormal esters decrease significantly because certain amounts of these esters are consumed in the side etherification reaction with epichlorohydrin (scheme 2).

The highest yields of chlorohydroxyalkyl esters were obtained at 75°C, when one of the reactants was used in excess (experiments 1,3,7 from table 3). The total amount of side products usually does not exceed few mol%. When an excess of acetic acid reported to epichlorohydrin is used (1.5/1) the yields of the two isomeric esters increase, but the regioselectivity of acetic acid addition to epi-

Sample	$V_{mesopore}$ (mL/g)	$V_{macropore}$ (mL/g)	S_{BET} (m^2/g)
Cr60Ce20Zr20	0.0788	0.5159	179.1
Cr40Ce40Zr20	0.0838	0.4281	193.48

Table 2
TEXTURAL PROPERTIES OF THE SYNTHESIZED MATERIALS

Sample	Catalyst	Temperature, K	Mole ratio	Reaction time, min	Yield of normal ester	Yield of abnormal ester
1	Cr60Ce20Zr20	348	1 : 1.15	360	69	13.07
2		348	1 : 1	450	65.44	12.16
3		348	1.5 : 1	420	70.96	15.15
4		338	1 : 1	300	42.55	8.68
5		338	1.5 : 1	300	53.15	11.99
6		368	1 : 1	180	42.28	9.55
7	Cr40Ce40Zr20	348	1.5 : 1	450	68.31	14.72
8		348	1 : 1	450	64.19	13.51
9		338	1.5 : 1	300	53.51	11.86
10		338	1 : 1	300	42.06	8.70

Table 3
EFFECT OF TEMPERATURE AND REACTANT MOLE RATIO

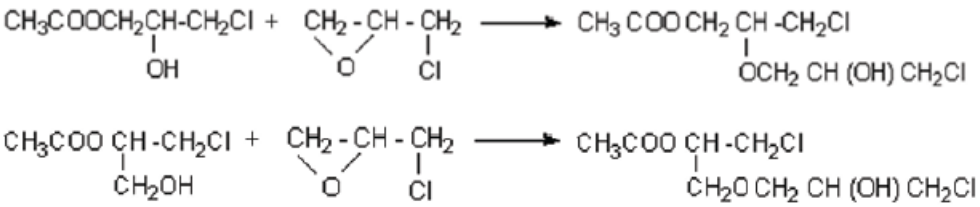

Scheme 2. The side reaction of etherification

chlorohydrin is disfavored. By using an epichlorohydrin/ acetic acid mole ratio of 1.15/1 both high yields in chlorohydroxyalkyl esters as well as a high regioselectivity are obtained.

Zeolites possess two kinds of catalytic acid sites Broensted and Lewis. It is generally considered that the most important from the catalytic point of view are the Bronsted acid sites known as structural hydroxyl groups.

The Broensted acidity is due to: (1) bridging hydroxyl groups Si(OH)M – protons are located on oxygen bridges connecting the tetrahedrally coordinated silicon and the metallic cation on framework position.The protons counterbalance the surplus of negative charge which occurs when Si atoms from the zeolite network are substituted by trivalent or divalent cations. The bridging hydroxyl groups M(OH)Si, which are located in the walls of the zeolitic cavities, constitute the strong acidic sites of protonic zeolites. In zeolites substituted with different metal atoms Si(OH)M, the acid strength of the hydroxyl protons depend on the chemical behaviour of the substituting atoms. The nature of these metal atoms influences the acid strength and, hence, the catalytic activity of substituted zeolites. In addition, the impact of the Si - O - M bond angle on the partial charge and the acid strength of the hydroxyl proton have to be considered; (2) OH groups from the external surface of zeolite particles (the free terminal silanol Si-OH or M-OH groups) originated from the framework defects. The acid strength of these Broensted centers is low; (3) formation of hydroxyl groups at the extra-framework metal species.

The ability to donate protons is not the only property of zeolites relevant to catalysis. These materials are also strong electron acceptors, phenomenon which is known as Lewis acidity. The Lewis acidity is attributed to vacant orbitals of: (1) metallic ions incorporated within the framework; (2) framework Lewis sites formed by framework dihydroxylation, (3) polyvalent metallic species which play the role of charge counterbalancing cations; (4) extra-framework M, O species (extraframework Lewis acid centers).

The basicity of zeolites is due to the Lewis centers associated with the O atoms of framework or to the Bronsted centers associated to hydroxyl groups. The strong Bronsted acids are conjugated to weak Bronsted bases, so that the existence of protons in zeolites is associated with basic sites. The nature and number of acid sites, their strength and distribution and also the accessibility towards the acid sites due to their various locations (for example, on the external surface or inside the narrow pores or in large and small cavities of the metallosilicate framework) are important for catalytic activity. The yeast cells used as template for the synthesized catalysts lead to obtaining of large macropores which facilitate the diffusion of reactants towards the catalytic sites. The increase of protons mobility with the rising of temperature is probably a reason for the enhancement of the addition reaction of chlorohydroxy-propyl esters to epichlorohydrin. We assume that the activation energies of the esterification and etherification reactions are not very different and at high temperature both reactions perform with closed reaction rates.

Reusability

The catalyst can be reused several times without loss of activity by simple seaparation from the reaction mixture (by sedimendation or filtration), followed by washing with ethylic alcohol and drying. The yields of chlorohydroxy-propyl esters remained constant even after ten uses.

Conclusions

The incorporation of heteroatoms within the silica framework has become a very efficient method forthe manufacturing of novel materials with improved mechanical, thermal and chemical properties. Some advantages such as ease of preparation, recovery by simple filtration at the end of reaction, lack of toxicity for environment make these materials suitable for a large number of applications in organic chemistry. ln this study we reported a general method for one-pot synthesis of metallosilicate macrospheres used as catalysts in the esterification reaction of acetic acid with epichlorohydrin. The effect of the working parameters on the yields of the two esters (3-chloro-2-hydroxypropyl acetate and 3-chloro-1-hydroxypropyl acetate) was investigated. The yield of 3-chloro-2-hydroxypropyl acetate is mainly affected by temperature (high temperatures favor the formation of abnormal ester). The mole ratio between acetic acid and epichlorohydrin (in the range studied) exerts a lower effect on the selectivity of reaction. The best results were obtained for the temperature of 75°C and the mole ratios between acetic acid and epichlorohydrin of 1 : 1.15 and 1.5 : 1.

References

1.SOROKIN, M.F., SHODE, L.G., KUZMIN, A.I., NOVIKOV, N.A., Izvestia VUZ-ov, Khimia I Khim Technol., 27, 1984, p. 658.
2.SHOLOGON, U.M., KLEBANOV, M.S., ALDOSHIN, V.A., KARPOV, O.N., Kinet. Katal., 26, 1985, p. 1059.
3.BUKOWSKA, A., GUSKOV, A., MAKAROV, M., ROCASZEWSKI, E., SVETS, V.F., J. Chem. Technol. Biotechnol., **63**, 1995, p. 374.
4.ZAKAVI, S., KARIMIPOUR, G.R., Catal. Commun., 10, 2009, p. 388.
5.BESPAL'KO, YU. N., SHVED, E.N., OLEINIK, N.M., Theoretical and Experimental Chemistry, 44, no. 5, 2008, p. 300.
6.KHALAFI NEZHAD, A., SOLTANI RAD, M.N., KHOSHNOOD, A., Synthesis, 16, 2003, p. 2552.
7.BUKOWSKI, W., J. Mol. Liq., **111**, no. 1-3, 2004, p. 47.
8.BUKOWSKA, A., BUKOWSKI, W., NOWOROL, J., J. Mol. Liq., **203**, no. 1-2, 2003, p. 95.
9.BUKOWSKA, A., BUKOWSKI, W., Org. Proc. Res. Dev., **6**, no. 3, 2002, p. 234.
10.BUKOWSKI, W., Int. J. Chem. Kinet., **32**, no. 6, 2000, p. 378.
11.JANIS, R., KREJCI, J., KLASEK, A., Eur. J. Lipid Sci. Technol., 102, no. 5, 2000, p. 351.
12.JACOBSEN, E.N., Acc. Chem. Res., **33**, 2000, p. 421.
13.READY, J.M., JACOBSEN, E.N., J. Am. Chem. Soc., **123**, 2001, p. 2687
14.ROSELIN,R.S., SELVIN,R., Chem. Eng. Commun., **199**, 2012, p. 221.
15.MURESAN, E.I., OPREA, S., MALUTAN, T., VATA, M., Cent. Eur. J. Chem., **5**, no. 3, 2007, p. 715.
16.MURESAN, E.I., DROBOTA, M., BARGAN, A., DUMITRIU, C.A.M., Cent. Eur. J. Chem., **12**, no. 4, 2014, p. 528.
17.FUXIANG, L., FENG, Y., YONGLI, L., RUIFENG L., KECHANG, X., Micropor. Mesopor. Mater., **101**, 2007, p. 250.
18.CARMONA, D., BALAS, F., SANTAMARIA, J., Mater. Res. Bull., **59**, 2014, p. 311.
19.OCAMPO, F., CUNHA, J.A., SANTOS DE LIMA, M.R., TESSONNIER, M.M., LOUIS, B., PEREIRA, B., Appl. Catal. A: General, **390**, 2010, p. 102.
20.VERNIMMEN, J., MEYNEN, V., COOL, P., Beilstein J. Nanotechnol., **2**, 2011, p. 785.
21.RATNASAMY, P., SRINIVAS, S., Catal. Today, **141**, 2009, p. 3.
22.VERNIMMEN, J., GUIDOTTI, M., SILVESTRE ALBERO, J., JARDIM, E.O., MERTENS, M., LEBEDEV, O.I., VAN TENDELOO, G., PSARO, R., RODRIGUEZ REINOSO, F., MEYNEN, V., COOL, P., Langmuir, **27**, 2011, p. 3618.
23.EIMER, G.A., DIAZ, I., SASTRE, E., CASUSCELLI, S.G., CRIVELLO, M.E., HERRERO, E.R., PEREZ PARIENTE, J. Appl. Catal., **343**, 2008, p. 77.
24.NAIK, B., GHOSH, N.N., Recent Patents on Nanotechnology, 3, 2009, p. 213.

25.KOSOVA, G., ERNST, S., HARTMANN, M., CEJKA, J., Eur. J. Inorg. Chem., 2005, p. 1154.
26.WANG, Z., JIANG, Y., RACHWALIK, R., LIU, Z., SHI, L., HUNGER, M., HUANG, J., ChemCatChem, 5, 2013, p. 1.
27.SARVI, M.N., STEVENS, G.W., LOUISE GEE, M., O'CONNOR, A.J., Micropor. Mesopor. Mater., **149**, 2012, p. 101.
28.CHEN, L.F., ZHOU, X.L., NORENA, L.E., WANG, J.A., NAVARETTE, J., SALAS, P., MONTOYA, A., DEL ANGEL, P., LLANOS, M.E., **253**, Appl. Surf. Sci., p. 2443.
29.LIU, F., WILHAMMAR, T., WANG, L., ZHU, L., SUN, Q. , MENG, X., CARRILO-CABRERA, W., ZOU, X., XIAO, F.S., J. Am. Chem. Soc., **134**, 2012, p. 4557.
30.DANILINA, N., CASTELANELLI, S.A., TROUSSARD, E., BOKHOVEN, J.A., Catal. Today **168**, 2011, p. 80.
31.VERBOEKEND, D., KELLER, T. C., MITCHELL, S., PÉREZ-RAMÍREZ, J., Adv. Funct. Mater., **23**, no. 15, 2013, p. 1923.
32.LI, K., VALLA, J., MARTINEZ, J.G., Chem. Cat. Chem., **6**, no. 1, 2014, p. 46.
33.VERNIMMEN, J., MEYNEN, V., MERTENS, M., LEBEDEV, O.L., TANDELOO, G.V., COOL, P., J. Porous Mater.,**19**, 2012, p. 153.
34.MOZGAWA, W., KROL, M., BARCZYK, K., Chemik, **65**, no. 7, 2011, p. 887.
35.LIZAMA, L.Y., KLIMOVA, E.T., J. Mater. Sci., **44**, 2009, p. 6617.
36.*** IUPAC Recommendations, Pure Appl. Chem., **66**, no. 8, 1994, p. 1739.
37.HAGYMASSY, J. JR., BRUNAUER, S., MIKHAIL, R.S., J. Colloid Interface Sci., **29**, no. 3, 1969, p. 485.
38.THOMMES, M., CYCHOSZ, K.A., Adsorption, **20**, 2014, p. 233.
39.MINTOVA, S., Micropor. Mesopor. Mater., **114**, 2008, p.1.

Manuscript received: 18.11.2015